Monte Carlo dose calculations for phantoms with hip prostheses

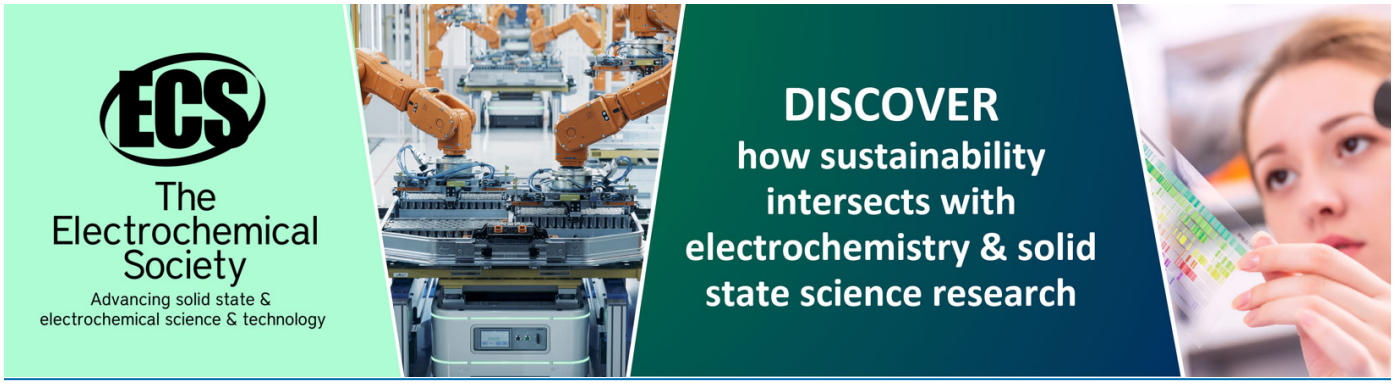

Journal of Physics: Conference Series **102** (2008) 012001 doi:10.1088/1742-6596/102/1/012001

Monte Carlo dose calculations for phantoms with hip prostheses

M. Bazalova[1], C. Coolens[2], F. Cury[3], P. Childs[2], L. Beaulieu[4], F. Verhaegen[1]

[1]Medical Physics Unit, Montreal General Hospital, McGill University, 1650 Cedar Avenue, Montreal, Quebec, H3G 1A4, Canada
[2]The Joint Department of Physics, Intsitute of Cancer Research and Royal Marsden NHS Trust, Sutton, SM2 5PT, UK
[3]Department of Oncology, Division of Radiation Oncology, McGill University, Montreal, Quebec, Canada
[4]Département de Radio-Oncologie et Centre de Recherche en Cancérologie de Université Laval, CHUQ Pavillon Hôtel-Dieu de Québec, Québec, Canada

Email: fverhaegen@medphys.mcgill.ca

Abstract. Computed tomography (CT) images of patients with hip prostheses are severely degraded by metal streaking artefacts. The low image quality makes organ contouring more difficult and can result in large dose calculation errors when Monte Carlo (MC) techniques are used. In this work, the extent of streaking artefacts produced by three common hip prosthesis materials (Ti-alloy, stainless steel, and Co-Cr-Mo alloy) was studied. The prostheses were tested in a hypothetical prostate treatment with five 18 MV photon beams. The dose distributions for unilateral and bilateral prosthesis phantoms were calculated with the EGSnrc/DOSXYZnrc MC code. This was done in three phantom geometries: in the exact geometry, in the original CT geometry, and in an artefact-corrected geometry. The artefact-corrected geometry was created using a modified filtered back-projection correction technique. It was found that unilateral prosthesis phantoms do not show large dose calculation errors, as long as the beams miss the artefact-affected volume. This is possible to achieve in the case of unilateral prosthesis phantoms (except for the Co-Cr-Mo prosthesis which gives a 3% error) but not in the case of bilateral prosthesis phantoms. The largest dose discrepancies were obtained for the bilateral Co-Cr-Mo hip prosthesis phantom, up to 11% in some voxels within the prostate. The artefact correction algorithm worked well for all phantoms and resulted in dose calculation errors below 2%. In conclusion, a MC treatment plan should include an artefact correction algorithm when treating patients with hip prostheses.

1. Introduction

Metal streaking artefacts in Computed Tomography (CT) can severely degrade image quality. CT images of patients with metal artefacts due to dental work, surgical clips or hip prostheses are often very difficult to contour. Moreover, it has been shown that metal streaking artefacts cause dose calculation errors in treatment planning systems taking heterogeneities into account[1], especially in those using Monte Carlo (MC) simulations[2]. Bazalova *et al.*[2] also show that in order to avoid large MC dose discrepancies, an artefact correction technique should be used when calculating the dose to

patients having hip prostheses. Another option to consider for patients having bilateral hip replacements is a prostate brachytherapy implant procedure.

Various artefact correction techniques are available to improve the image quality. The two main approaches for correction of metal artefacts are iterative techniques[3] and techniques based on modified filtered back-projection[4]. Modified filtered-back projection techniques result in a slightly lower image quality than iterative techniques, nevertheless, they are used for their shorter computation time. A technique based on modified filtered back-projection using cubic interpolation is used in this work. The technique is described in detail elsewhere[2]. It basically involves interpolation of corrupted sinogram data corresponding to metallic objects using adjacent projections and cubic interpolation. The method works very well for simple prosthesis geometries. For complex prosthesis geometries, the algorithm corrects the large artefacts and results in formation of minor streaks. It has to be noted that an alternative approach to more accurate treatment of patients with hip prostheses is the use of the extended CT-scale as demonstrated by Coolens and Childs[5].

In this work, we evaluated the effect of three common hip prosthesis materials on the extent of metal streaking artefacts and their influence on MC dose calculation. We also applied a sinogram interpolation method based on cubic splines on the original CT images, obtained artefact-corrected CT geometries and evaluated the effect of the correction on MC dose calculations.

2. Materials and methods

One or two prostheses made of three common prosthesis materials were placed in a 27 cm diameter cylindrical acrylic phantom filled with water. This allowed us to construct unilateral and bilateral hip prosthesis pelvic phantoms.

2.1. Prosthesis materials

The elemental compositions of the three common hip prosthesis materials[6] are listed in table 1. Ti-alloy with the lowest mass density (4.48 g/cm^3) produces the least artefacts. Co-Cr-Mo alloy with 8.20 g/cm^3 creates the most artefacts, as shown in figure 1 where phantom CT images and photographs of the prostheses are presented. As can be seen in figure 1b, a solid steel acetabular cup is a part of the stainless steel prostheses. Ceramic acetabular cups can be placed on the stem of the Ti-alloy and Co-Cr-Mo alloy prostheses, however, they were not used in our experiments.

Table 1. Elemental composition (fraction by weight) and mass densities (ρ) of three common hip prosthesis materials.

Ti-alloy ρ=4.48 g/cm^3		Stainless steel ρ=6.45 g/cm^3		Co-Cr-Mo alloy ρ=8.20 g/cm^3	
Ti	89.17	Fe	62.72	Co	61.90
Al	6.20	Cr	21.00	Cr	28.00
V	4.00	Ni	9.00	Mo	6.00
Fe	0.30	Mn	3.60	Mn	1.00
O	0.20	Mo	2.50	Si	1.00
C	0.08	Si	0.75	Fe	1.00
N	0.05	N	0.43	Ni	0.75
				C	0.35

2.2. Scanning parameters and artefact correction

The hip prosthesis phantoms were scanned on a PQ5000 single slice CT scanner (Royal Philips Electronics, Eindhoven, the Netherlands). The axial mode was chosen to acquire 5 mm thick slices at 5 mm separation, 130 kVp and 400 mAs. Moreover, a 100 kVp scan of the Ti-alloy bilateral phantom

was taken and the effect of tube voltage on metal artefacts was evaluated. All scans consisted of 24 images with 512x512 pixels. The pixel size was determined by the 48 cm field size to be 0.94 mm.

The phantom raw data were saved in the scanner and transferred via a modem connection to a PC for processing. The raw data consisted of 512 detector readings at 2400 x-ray tube positions and were subsequently converted to sinograms. The sinogram interpolation correction algorithm based on cubic spline interpolation was run for each slice on a 1.6 GHz PC in Matlab (The Mathworks, Natick, MA). The correction of one slice took approximately 11 minutes.

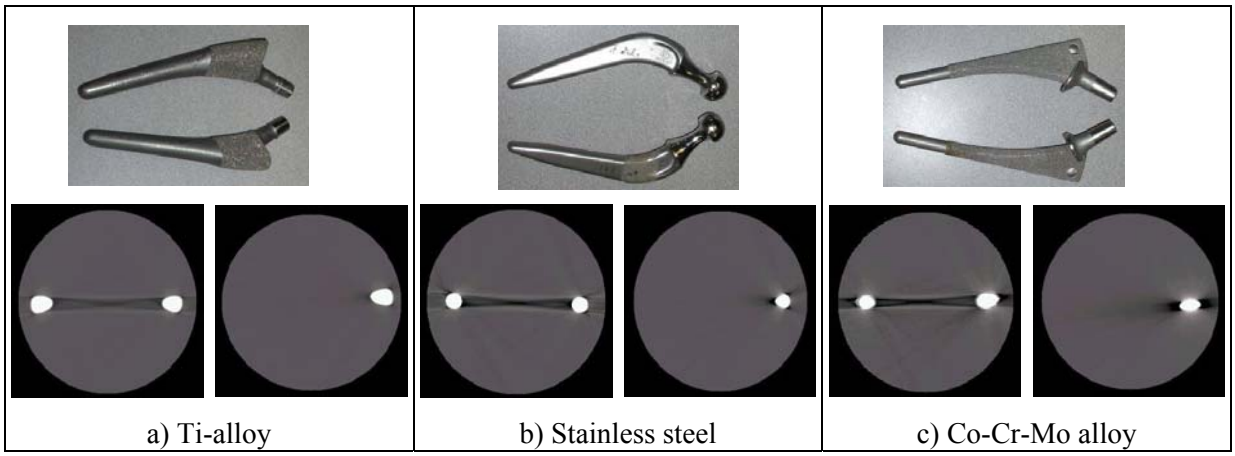

Figure 1. Photographs of three common types of hip prostheses and the extent of artefacts produced by them in bilateral and unilateral prosthesis water phantoms.

2.3. Treatment plan

The original CT images of the bilateral steel prosthesis phantom with metal streaking artefacts were transferred to a contouring station and a physician was asked to create a prostate case by delineating a fictitious prostate (target) and rectum (organ at risk). The CT images with the contours were then transferred to a planning station and the external contour of the phantom was semi-automatically drawn. The automatic external contour detection of the surface of the phantom failed due to the presence of metal artefacts and the contouring had to be completed manually. The geometry of the steel bilateral prosthesis phantom is presented in figure 2. The external contour is drawn in blue, steel prostheses in black, the prostate in red and the rectum in green. The prostate volume is 42.8 cc.

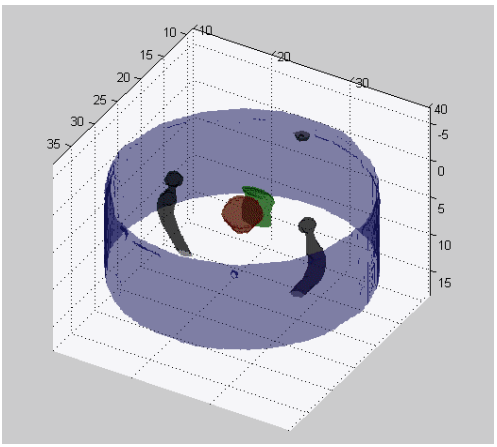

Figure 2. Phantom geometry – external contour (blue), steel prostheses (black), prostate (red), and rectum (green).

Subsequently, a dosimetrist generated a treatment plan. A five 18 MV co-planar photon beam arrangement was chosen as it is commonly used for prostate treatments in our hospital. Since the prostheses were relatively small, a setup with all beams missing the prosthesis could be used. The

beam angles were 300°, 230°, 0° (using IEC convention), 60°, and 130° with field sizes being 5.5 cm in *x* and 8.0 cm in *y* which spared the rectum. The treatment plan was then applied to all phantoms.

2.4. Monte Carlo dose calculations

The beam arrangement from the planning station was implemented in the EGSnrc/DOSXYZnrc[7] Monte Carlo code. The CT images of the phantom were used to create three sets of geometry files in the following way. First, the exact geometry was built on the basis of the original CT images by assigning the voxels with the maximum CT number (or Hounsfield unit, HU, 3095 for our scanner where HU = 0 for water) to the corresponding prosthesis material. The remaining voxels of the phantom were assigned to water with mass density 1.0 g/cm^3.

Secondly, the original CT geometry and the corrected geometry were created on the basis of the original CT images and the artefact-corrected images, respectively. Similarly to the exact geometry, the 3095 HU voxels were assigned to the corresponding prosthesis material. Remaining voxels in the phantom were assigned to water, including the voxels with the low CT numbers due to the artefacts. The mass densities were assigned on the basis of the scan and a (HU,ρ) calibration curve. The calibration curve was obtained using scans of an RMI electron density calibration phantom (Gammex, Middleton, WI) taken at the corresponding tube voltage.

Note that the contouring of the prostheses was done using a simplistic approach that assigns the saturated HU to the corresponding prosthesis material. However, since identical prosthesis contours were used in all three geometries (in the exact, original CT and in the artefact-corrected geometry), the dose distributions are consistent and the dose differences are not compromised by the prosthesis geometries. The exact prosthesis geometry could be found by applying the filtered back-projection on the raw data and using a pre-defined windowing and levelling[5].

The acrylic cylinder was excluded from the geometry. As can be seen in figure 2, the prostate is very close to the top of the phantom. This geometry might result in a lack of scattered radiation. In order to account for the scatter, a 10 cm layer of uniform water was added on top of the phantom in all geometries.

Three dose calculations were performed for each of the phantom geometries: in the exact geometry (D_{ex}), in the original CT geometry (D_{or}), and in the artefact-corrected geometry (D_{cor}). The resulting dose distributions were compared. The calculations were run with 1×10^9 particles with the energy cut-offs of 10 keV for both photons and electrons. The dose to air was set to zero , as is commonly done in MC dose calculations.. The dose calculation uncertainty in high dose regions did not exceed 1.2%.

3. Results

The results are presented in two different ways. In order to evaluate the effect of the artefact correction algorithm on the image quality, the original CT images and the artefact-corrected images of the isocentric slice are displayed. Percentage dose difference maps of the isocentric slice are also plotted. The dose difference map in the original geometry is calculated as $(D_{ex}-D_{or})/D_{ex}$ and in the artefact-corrected geometry as $(D_{ex}-D_{cor})/D_{ex}$.

3.1. Bilateral prosthesis phantoms

All bilateral prosthesis phantoms contained severe artefacts. The most severe artefacts were observed for the high density Co-Cr-Mo alloy (figure 3). Figure 3a shows the large extent of the artefacts and it can be seen clearly that the prostate (in red) is contoured in the area where the streaks are the most pronounced. The artefact-corrected image produced using the sinogram interpolation method is presented in figure 3b where the large artefacts between the prostheses are completely corrected. Note that minor streaks in the vicinity of the prostheses appeared which is fairly typical for the sinogram interpolation correction algorithm. The dose difference maps of the original geometry and the artefact-corrected geometry with respect to the exact geometry are plotted in figure 3c and 3d, respectively. The artefact-affected area of figure 3c is enlarged in figure 3e. Note that the scale is also enlarged in figure 3e.

As can be seen in figure 3e, some voxels have dose calculation errors larger than 15%. This comes from the fact that dose to air was set to zero in the DOSXYZnrc calculation. When this option is chosen, the dose to artefact-affected voxels with density < 0.044 g/cm^3 is zeroed, which results in dose differences close to 100%. Figure 3e also contains non-air voxels with dose calculation errors from -3% up to 11% in the prostate volume that are entirely caused by the metal streaking artefacts. Since the rectum is contoured outside the artefacts for all phantoms, the dose differences in the rectum are within 2% for all phantom geometries. Figure 3d demonstrates that MC dose calculations are improved in the artefact-corrected geometry. The dose calculation errors are within 2% and reflect statistical uncertainties of the calculation.

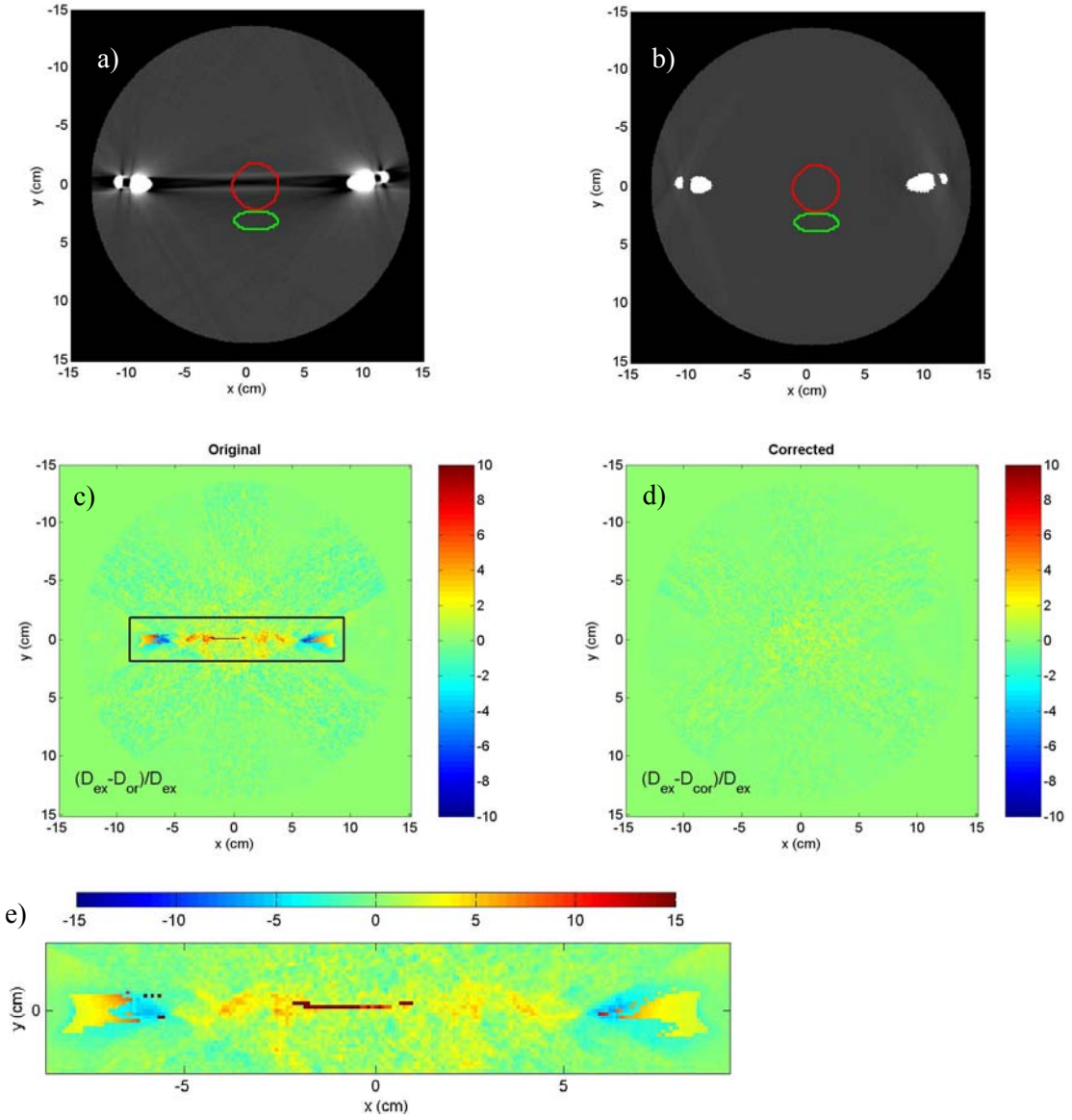

Figure 3. CT images of the original geometry (a) and the artefact-corrected geometry (b) for the Co-Cr-Mo alloy bilateral prosthesis phantom. Differences in dose distribution from the exact geometry for the original CT geometry (c) and the artefact-corrected geometry (d). The artefact-affected volume marked by the black rectangle of (c) is enlarged in (e).

The remaining results for the Ti-alloy and the steel prosthesis phantoms are not shown, however, the maximum dose errors in voxels with density > 0.044 g/cm^3 were found to be 3% and 5%, respectively. The correction algorithm produced geometries with suppressed metal artefacts that resulted in dose difference maps with dose calculation errors within 2%.

3.2. Unilateral prosthesis phantoms

The results for the Co-Cr-Mo unilateral prosthesis phantom are shown in figure 4. The original CT image and the artefact-corrected image of the isocentric slice are displayed in figure 4a and 4b, respectively. As expected, artefacts produced by one Co-Cr-Mo prosthesis are less severe than artefacts produced by two Co-Cr-Mo prostheses. Nevertheless, streaks are spread in the entire phantom. The correction algorithm works well and corrects for the main artefacts (figure 4b).

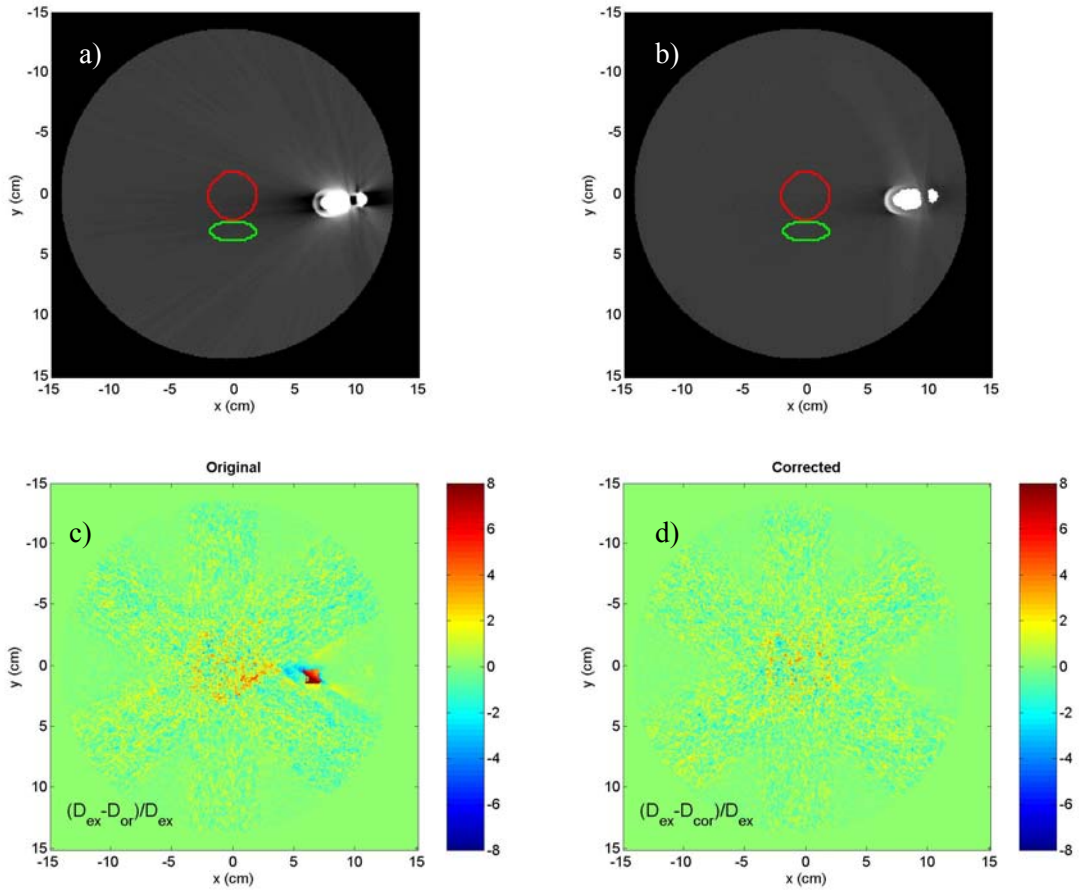

Figure 4. CT images of the original geometry (a) and the artefact-corrected geometry (b) for the Co-Cr-Mo unilateral prosthesis phantom. Dose distribution differences from the exact geometry for the original CT geometry (c) and the artefact-corrected geometry (d).

Since one of the five 18 MV photon beams does not miss the small volume affected by the artefacts, the dose distribution in the original geometry is affected by the streaking artefacts. Dose uncertainties up to 3% are observed close to the right prosthesis in the original CT geometry (figure 4c). The rest of dose difference map for the original geometry and the entire dose difference map for the artefact-corrected geometry (figure 4d) reflect mostly the dose calculation uncertainties.

It should be noted that the direction of the 130° beam that passes through the artifact affected volume should not be changed. It could be only changed in the clockwise direction which would result in excessive dose to the rectum.

The results for the unilateral Ti-alloy phantom and the steel phantom are not presented. The artefact-affected volume for these prostheses is small. Therefore, the photon beams miss the volume affected by the streaking artefacts. As a result, the dose distribution in the original geometry is very similar to the dose distribution in the exact geometry and in the artefact-corrected geometry. The dose difference maps are very similar and reflect only the dose calculation uncertainties.

3.3. Effect of tube voltage

The effect of tube voltage on the extent of metal streaking artefacts was studied on the bilateral Ti-alloy phantom. A scan at 100 kVp produced significantly more artefacts than the scan at 130 kVp. The maximum dose difference from the exact geometry increased from 3% for the 130 kVp geometry to 5% for the 100 kVp geometry within the prostate volume. The artefact correction algorithm worked again very well and the dose distribution in the artefact-corrected geometry was in agreement with the exact geometry dose distribution. As our example demonstrates, higher tube voltages should be used for patients with hip prostheses, if possible.

4. Conclusion

We have evaluated the effects of metal streaking artefacts produced by three common hip prosthesis materials on Monte Carlo dose calculations for a hypothetical five 18 MV photon beam prostate treatment. Unilateral and bilateral Ti-alloy, stainless steel, and Co-Cr-Mo prosthesis phantoms with a fictitious prostate and rectum were studied. A sinogram interpolation method for correction of metal artefacts was applied on all phantoms and the effect of the correction on MC dose calculations was also evaluated.

It was found that bilateral hip prosthesis phantoms show significant streaking artefacts for all hip prosthesis materials. The largest dose discrepancies due to the artefacts were observed for the high density Co-Cr-Mo bilateral phantom. The dose calculation errors from the exact geometry were as high as 11% in the prostate volume. The dose calculation errors for the bilateral Ti-alloy and steel prosthesis phantoms were 3% and 5%, respectively.

Unilateral prosthesis phantoms show less streaking artefacts than bilateral prosthesis phantoms. Therefore, in the case of the unilateral low density (steel and Ti-alloy) prosthesis phantoms, it is possible to choose a beam arrangement that misses the artefact affected volume. As a result, the calculated dose distributions are not affected by the presence of the artefacts which strongly depends on the size of the prosthesis and the patient geometry. However, artefacts in the phantom with the high density Co-Cr-Mo prosthesis were more pronounced and the beam close to the prosthesis could not avoid the artefact-affected volume. This caused a 3% dose discrepancy from the exact geometry.

The effect of tube voltage on the extent of artefacts was studied for the bilateral Ti-alloy phantom. It was found that in order to decrease dose calculation errors (assuming no artefact correction algorithm), higher tube voltages should be used when scanning patients with bilateral hip prosthesis. However, when the artefact correction algorithms based on interpolation of sinograms are used, the effect of tube voltage is insignificant.

The sinogram interpolation correction algorithm performed well in all phantom geometries which resulted in dose calculations errors below 2%. We conclude that in order to avoid large dose discrepancies, Monte Carlo treatment planning for bilateral hip prosthesis patients should always include a metal artefact correction algorithm. If one or more beams pass through the artefact-affected volume, a correction algorithm for metal streaking artefacts should be also used for patients with one hip prosthesis.

Acknowledgement
The authors would like to thank to Dr. Gabriela Stroian for generating the prostate treatment plan and to Robin van Gils for making the phantom. The work has been supported by Grant No. 206358 from the Natural Science and Engineering Research Council of Canada (NSERC). F.V. is a Research Scientist supported by the Fonds de Recherche en Santé du Québec (FRSQ).

References

[1] Kim Y, Tomé W A, Bal M, McNutt T R, Spies L 2006 The impact of dental metal artifacts on head and neck IMRT dose distributions *Radiother. Oncol.* **79** 198-202
[2] Bazalova M, Beaulieu L, Palefsky S and Verhaegen F 2007 Correction of CT artifacts and its influence on Monte Carlo dose calculations *Med. Phys.* **34** 2119-2132
[3] Wang G, Snyder D L, O'Sullivan J A and Vannier M W 1996 Iterative Deblurring for CT Metal Artefact Reduction *IEEE Transitions on Medical Imaging* **15** 657-664
[4] Yazdi M, Gingras L and Beaulieu L 2005 An adaptive approach to metal artefact reduction in helical computed tomography for radiation therapy treatment planning: experimental and clinical studies *Int. J. Radiat. Oncol., Biol., Phys.* **62** 1224–1231
[5] Coolens C and Childs P J 2003 Calibration of CT Hounsfield units for radiotherapy treatment planning of patients with metallic hip prostheses: the use of the extended CT-scale *Phys. Med. Biol.* **48** 1591-1603
[6] Reft C, Alecu R, Das I J, Gerbi B J, Keall P, Lief E, Mijnheer B J, Papanikolaou N, Sibata C and Van Dyk J, AAPM Radiation Therapy Committee Task Group 63 2003 Dosimetric considerations for patients with HIP prostheses undergoing pelvic irradiation. Report of the AAPM Radiation Therapy Committee Task Group 63 *Med. Phys.* **31** 1162–1182
[7] Walters B R B and Rogers D W O 2007 DOSXYZnrc Users Manual *NRCC Report No. PIRS 794revB*